Mechanism of Quenching of SO_2 $\tilde{C}(^1B_2)$ by He, Ar, and N_2

Takefumi Oka
Nagaoka Technical College, Nagaoka, Niigata 940

(Received May 23, 1983)

Sulfur dioxide gas was excited to $\tilde{C}(^1B_2)$ state by steady illumination and the total intensity and the spectrum of the fluorescence were measured in the SO_2 pressure range of 0.1—1 Torr (1 Torr≈133.322 Pa) both in the absence and in the presence of He, Ar, and N_2 up to 600 Torr. The observed fluorescence spectrum was broad but the wavelength of the maximum intensity was found to be dependent upon excitation wavelength in the range of 240—220 nm. Addition of foreign gases caused the blue shift of the fluorescence spectrum. The Stern-Volmer plots were nonlinear for quenching by the foreign gases but linear for self-quenching. It was suggested that the foreign gas molecules cause not only vibrational deactivation but also collision induced transition between $^1B_2$ state and a nonemitting state and that the rate constants of the transition to the nonemitting state are larger from higher vibrational levels than from lower ones.

Sulfur dioxide has three absorption systems in the ultra-violet region. The first weak absorption system ($400>\lambda>340$ nm) is due to $\tilde{a}(^3B_1)$ state and plays an important role in photochemistry in the lower atmosphere. The second system ($340>\lambda>250$ nm) consists of a banded structure due to $\tilde{A}(^1A_2)$ state and an underlying continuum due to $\tilde{B}(^1B_1)$ state. The fluorescence from this system shows nonexponential decay, indicating a strong coupling of $\tilde{A}(^1A_2)$ with $\tilde{B}(^1B_1)$. These two systems have been extensively studied.[1-4,13,18] On the other hand, only a few studies have been reported about the third system ($250>\lambda>175$ nm). A group of absorption bands in this system was once classified into two electronic states, α_1 and α_2 by Duchesne and Rosen[5] ($\tilde{C}$ and $\tilde{D}$ in Herzberg's summary[6]). Recently Brand and his co-workers have assigned these bands to one electronic state $^1B_2$ on the basis of the rotational analysis.[7-9]

Okabe examined absorption and fluorescence excitation spectra of this system and suggested the occurrence of predissociation below 220 nm.[10] He estimated quenching rate constant of one of the bands (at 220.6 nm in Fig. 2) by Ar to be 5×10^{-11} cm^3 molecule^{-1} s^{-1} by the intensity reduction on addition of Ar of 400 Torr assuming Stern-Volmer mechanism.

Hui and Rice studied the decay of the ten vibronic bands between 230 and 210 nm and observed simple exponential decay.[11] They measured the lifetimes and quantum yields of the fluorescence. The quantum yield was nearly unity at longer wavelengths, but decreased as wavelength approached to 220 nm and dropped abruptly below 220 nm. This abrupt change supports the occurrence of the predissociation below 220 nm. Observed radiative lifetimes were 30—50 ns while a lifetime calculated from the oscillator strength was 9 ns.

Very recently, quantum beat in the decay of $^1B_2$ due to the coupling with the ground electronic state was observed in a supersonic free jet.[12] As for fluorescence emission spectrum, only a broad spectrum centered at 320 nm was reported.[13,14]

In the present paper, the experimental results of self-quenching and foreign gas quenching will be presented and collision induced coupling of $^1B_2$ state with another state will be suggested.

Experimental

The sample gases were handled in a conventional vacuum line with a mercury diffusion pump. Pressure was measured with a mercury manometer and an oil manometer.

The excitation light beam was obtained with a combination of Ushio 500W Xenon lamp and Ritsu MC-20L monochromator, and passed through a T-shaped fluorescence cell along the principal axis. The geometric size of the cell with three quartz windows is shown in Fig. 1. The outside wall of the cell excluding the windows was painted black. The intensity of the transmitted light was monitored with a photomultiplier (1p28) behind the cell.

The emission was observed through a side window of the cell with an uncooled photomultiplier(HTV R585). The total intensity observed without any optical filters was used for quenching study. The excitation bandpass($\Delta\lambda_{ex}$) was 0.2 nm. The length of the view zone along the principal axis of the cell was about 3 cm (Fig. 1). For the measurements of fluorescence spectra, the second monochromator (JASCO CT-25N) was placed in front of the side window of the cell. The bandpasses used were $\Delta\lambda_{ex}=4$ nm for the excitation monochromator and $\Delta\lambda_{em}=9$ nm for the emission monochromator. The quantum efficiency of R585 was not constant over the range of 250—400 nm.[15] However, the correction for this effect did not affect the foreign gas quenching data.

A photon counter (HTV-C767) was used to count the number of photons emitted. The output of the counter and the 1p28 photomultiplier was fed into a two pen strip chart recorder. The nominal emission intensities were corrected for variation of the intensity of the excitation beam by using the intensity monitored with 1p28.

Sulfur dioxide synthesized from Na_2SO_3 and H_2SO_4 was bubbled through H_2SO_4, dryed over P_2O_5 and distilled *in vacuo* at −80 °C.

Helium, argon, and nitrogen used here were of purity

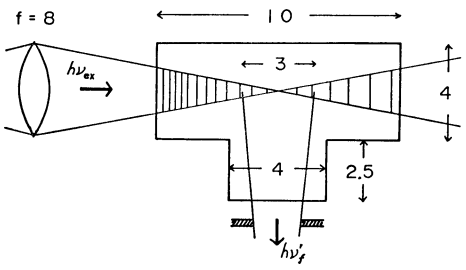

Fig. 1. Fluorescence cell. The unit of length is cm.

higher than 99.99% and passed through a liquid nitrogen trap before use. In the foreign gas quenching study, the cell was first filled with a certain pressure of SO_2 (mostly 0.8 Torr) and then a foreign gas of higher pressure (than 10 Torr) was added. The homogeneity of the mixture was confirmed by comparing the results obtained by this method with those of premixed sample. All the experiments were done at room temperature.

Results

Figure 2 shows the excitation spectrum of 0.9 Torr of SO_2 in the optical range of 240—216 nm. The vibrational assignment indicated in the figure is according to Brand.[6,8]

The bands located at wavelengths shorter than 225 nm could not be expressed by a combination of three normal modes because of the coupling of ν_1' and ν_3'. Quenching experiments were done with the resolved bands shown in Fig. 2. The emission spectra of 0.8 Torr SO_2 excited at various wavelengths are shown in Fig. 3. The emission spectra seemed to have structure[16] but the optical resolution in the present work ($\Delta\lambda_{ex}=4$ nm, $\Delta\lambda_{em}=9$ nm) was not high enough to resolve them. When the exciting light was changed to the longer wavelengths, the spectrum shifted to the blue.

The change of the emission spectrum due to the variation of SO_2 pressure from 0.1 to 1 Torr was negligibly small compared to that due to the high pressure foreign gas (*vide infra*). Foreign gas quenching of fluorescence excited at each vibronic band is shown in Fig. 4 for He, Fig. 5 for Ar, and Fig. 6 for N_2. The

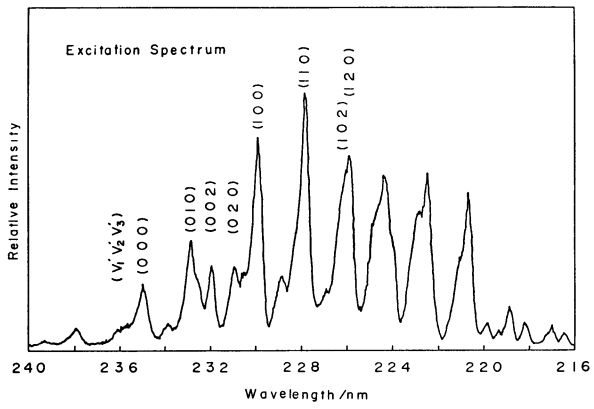

Fig. 2. Fluorescence excitation spectrum of $\tilde{C}^1B_2$ state. $p(SO_2)=0.9$ Torr and $\Delta\lambda_{ex}=0.2$ nm. The three figures in a parenthesis are a set of the vibrational quantum number of $^1B_2$ state, (v_1', v_2', v_3').

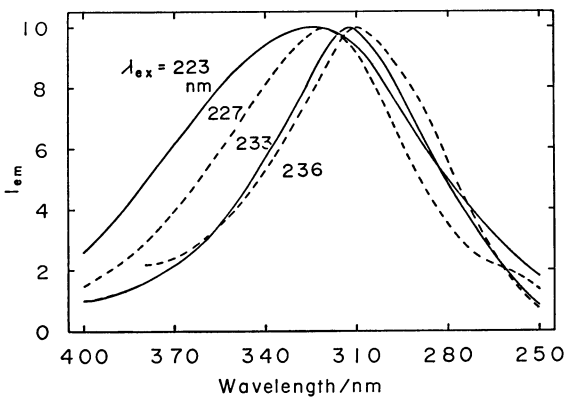

Fig. 3. Emission spectra excited at various wavelengths (λ_{ex}). $p(SO_2)=0.8$ Torr, $\Delta\lambda_{ex}=4$ nm, and $\Delta\lambda_{em}=9$ nm. Spectra were not corrected for wavelength dependent sensitivity of the detection system.

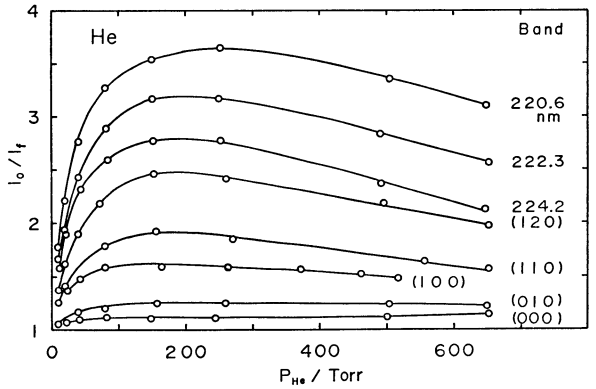

Fig. 4. Fluorescence quenching by He. $\Delta\lambda_{ex}=0.2$ nm and $p(SO_2)=0.8$ Torr. For the upper three curves, the bands are indicated by the wavelengths. I_f and I_0 are the fluorescence intensities with and without He, respectively.

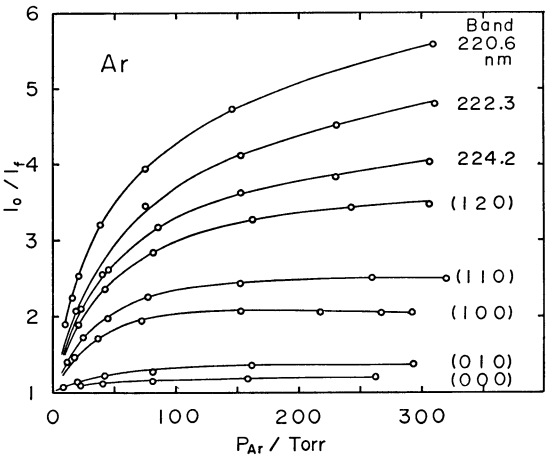

Fig. 5. Fluorescence quenching by Ar. See the legand of Fig. 4.

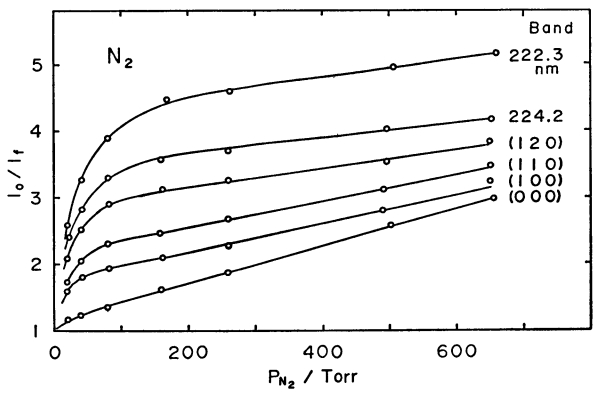

Fig. 6. Fluorescence quenching by N_2. See the legand of Fig. 4.

plots of I_0/I_F vs P_M are nonlinear, indicating that the quenching mechanism is not Stern-Volmer type.

As the foreign gas pressure increased from zero to about 200 Torr, intensity of emission decreased rapidly for all three gases. Above 200 Torr, the emission intensity showed different pressure dependence for the three gases, the intensity gradually increased for He, leveled off for Ar, and gradually decreased for N_2.[17]

The effects of addition of N_2 on the emission spectrum were the blue shift of the wavelength of emission maximum and the narrowing of the emission band width (Figs. 7-a,b).

The wavelength of maximum seems to converge to about 305 nm at the high pressure limit. The extent of the blue shift was large upon the excitation at shorter wavelengths.

The effects of addition of He and Ar on emission spectrum were similar to that of N_2. No difference among the three gases was observed upon the excitation at 233 nm. On the excitation at 223 nm, the efficiency of the effect decreased in the order of N_2, He, and Ar.

The self-quenching results of (110) band are compared in Fig. 8 for the cases in the absence and in the presence of high pressure argon. With Stern-Volmer mechanism, the straight lines with the same intercepts and with different slopes (larger in Ar) are expected. The plots in Fig. 8 show straight lines. However, the slope and the intercept in the presence of Ar are larger than those in the absence of Ar, though the difference in the intercepts is small. When He and N_2 were used in place of Ar, similar results were obtained. Table 1 summarizes the ratios of both the slope and the intercept in the presence of a foreign gas of about 200 Torr to those in the absence of the foreign gas.

Self-quenching was examined for each vibronic band of pure SO_2 in the SO_2 pressure range of 0.1—4 Torr. Self-quenching constants were determined as the ratio of intercept to slope in a plot of the type of Fig. 8 and are listed in the 2nd column of Table 3.

Discussion

Since the emission spectra were different for the excitation at different wavelengths as shown in Fig. 3, it can be said that the emitting species in pure SO_2 of 0.1—1 Torr is not vibrationally thermalized before the emission of fluorescence.

The blue shift of the emission spectra on the addition of the foreign gases can be interpreted as vibrational relaxation because the change of excitation level from higher to lower also caused the blue shift of the emission spectrum (Figs. 3 and 7). Since in the foreign gas quenching (Figs. 4—6) the rapid decrease followed by leveling off of the emission intensity as the foreign gas pressure increases from 0 to about 200 Torr is common to all the three gases, we may assume that

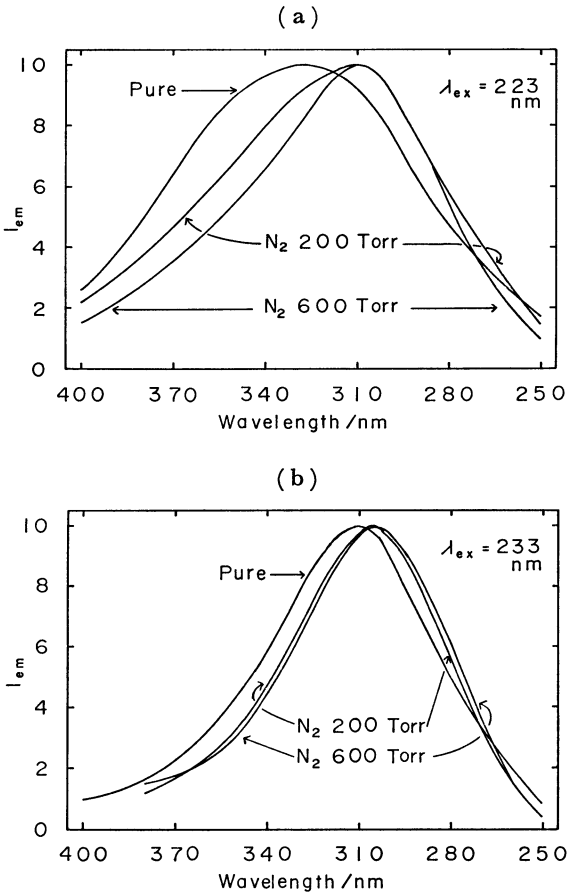

Fig. 7. Effect of addition of N_2 on the emission spectrum. $p(SO_2)=0.8$ Torr, $\Delta\lambda_{ex}=4$ nm, and $\Delta\lambda_{em}=9$ nm. a) $\lambda_{ex}=223$ nm, b) $\lambda_{ex}=233$ nm.

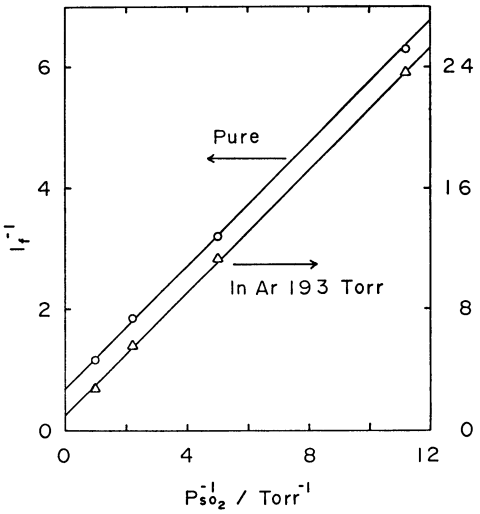

Fig. 8. Effect of Ar on self-quenching of (110) band. $\Delta\lambda_{ex}=0.2$ nm. I_f is corrected for the nonlinarity with respect to $p(SO_2)$.

TABLE 1. EFFECTS OF FOREIGN GASES ON SELF-QUENCHING OF (110) BAND

Foreign gas, M[a]	Intercept ratio[b]	Slope ratio[b]
He	1.1±0.1	2.9±0.1
Ar	1.3±0.1	4.2±0.1
N_2	1.4±0.1	4.1±0.1

a) $p(M)=200$ Torr and $p(SO_2)=0.1$—1.0 Torr. b) The intercept and the slope are those in the plot of $1/I_f$ *vs.* $1/p(SO_2)$.

this pressure dependence reflects the main structure of the foreign gas quenching mechanism.

Therefore, the mechanism we look for must be able to explain the following three features.

1) Foreign gases cause vibrational relaxation.

2) Fluorescence intensity decreases as foreign gas pressure increases and levels off above 200 Torr.

3) In the self-quenching, the plot of $1/I_f$ against reciprocal of SO_2 pressure is linear, and its slope is much larger in the presence of the foreign gas than in the absence of it while its intercept is only slightly larger in the presence of foreign gas.

First of all, we examine the equations for self- and foreign gas quenching expected with Stern-Volmer mechanism.

$$S + h\nu \xrightarrow{I_a} S^* \ (^1B_2, v'),$$
$$S^* \xrightarrow{k_r} S + h\nu'$$
$$S^* + S \xrightarrow{k_q} \text{self-quenching},$$
$$S^* + M \xrightarrow{k_m} \text{foreign gas quenching},$$

where S and M denote SO_2 and foreign gas molecules, respectively. I_a is the light intensity absorbed by SO_2 molecules at the view zone in the cell and is proportional to both the concentration of SO_2 and the incident light intensity I_l.

$I_a=\alpha I_l[S]$, where α is a proportional constant. Then the fluorescence intensity I_F is

$$I_F = k_r[S^*].$$

This mechanism leads to the equations;

$$I_0/I_f = 1 + \{k_m[M]/(k_r+k_q[S])\}, \quad (1)$$
$$1/I_f = [k_q+\{(k_r+k_m[M])/[S]\}]/(\alpha k_r), \quad (2)$$

where $I_f=I_F/I_l$, the fluorescence intensity relative to the incident light intensity, and I_0 is the value of I_f at $[M]=0$. Equation 2, when plotted I_f^{-1} *vs.* $[S]^{-1}$, gives a straight line with a slope $(k_r+k_m[M])/(\alpha k_r)$ and an intercept of $k_q/(\alpha k_r)$, and can explain the experimental results except for the slight dependence of the observed intercept on [M]. Equation 1 represents a straight line with a slope of $k_m/(k_r+k_q[S])$ in the plot of I_0/I_f *vs.* [M], while the experimental curves in Figs. 4—6 have slopes of decreasing functions of [M]. The vibrational relaxation is neither expected in this mechanism.

In the above mechanism, k_m is supposed to be a constant. However, if we would expect this mechanism to describe the experimental results, the slope, $k_m/(k_r+k_q[S])$, expected from Eq. 1 must be a decreasing function of [M] which approaches to zero at high pressure limit. We may attribute this [M] dependence to k_m. Secondly tested is the mechanism where vibrational relaxation takes place along with quenching processes. Higher vibrational levels are assumed to have larger quenching rate constants (k_m) than lower levels do. If Eq. 1 is applied to this system, the apparent k_m obtained would decrease as [M] increases because of vibrational relaxation. The following processes represent such a model where for simplicity only two levels are assumed.

$$S + h\nu \xrightarrow{I_a} S^*(1),$$
$$S^*(1) \xrightarrow{k_r} S + h\nu',$$
$$S^*(1) + S \xrightarrow{k_q} \text{self-quenching},$$
$$S^*(1) + M \xrightarrow{k_{m1}} \text{quenching}$$
$$\xrightarrow{k_v} S^*(0) + M,$$
$$S^*(0) \xrightarrow{k_r} h\nu' + S,$$
$$S^*(0) + S \xrightarrow{k_q} \text{self-quenching},$$
$$S^*(0) + M \xrightarrow{k_{m0}=0}$$
$$(k_{m1}>k_{m0}=0),$$

where $S^*(1)$ and $S^*(0)$ represent $v'=1$ and $v'=0$ levels of $^1B_2$ state respectively. The value of k_{m0} must be taken as zero otherwise emission intensity would not level off at high pressure of M. This mechanism leads to the Eqs. 1′ and 2′ below.

$$I_0/I_f = 1+\{k_m'[M]/(k_r+k_q[S])\}, \quad (1)'$$
$$k_m' = k_{m1}(k_r+k_q[S])/(k_r+k_q[S]+k_v[M]),$$

and when $k_q[S] \ll k_r+k_v[M]$,

$$1/I_f = [k_q\{1+k_{m1}k_v[M]^2/(k_r+k_v[M])^2\} + k_r\{1+k_{m1}[M]/(k_r+k_v[M])\}/[S]]/(\alpha k_r). \quad (2)'.$$

This mechanism explains the first and second features but cannot explain the third feature because Eq. 2′ requires the slope and intercept in self-quenching increase by the same factor of $1+(k_{m1}/k_v)$ on addition of sufficiently high pressure of M. The origin of the failure of this mechanism is zero value of k_m at the lowest level. For the mechanism to be able to explain the third feature, k_m must be nonzero and yet be a decreasing function of [M].

Then we hope to realize this situation by adding a back reaction of quenching process to the Stern-Volmer mechanism as follows;

$$S + h\nu \xrightarrow{I_a} S^*(^1B_2),$$
$$S^* \xrightarrow{k_r} S + h\nu',$$
$$S^* + S \xrightarrow{k_q} \text{self-quenching},$$
$$S^* + M \underset{k_m'}{\overset{k_m}{\rightleftarrows}} S^{**} + M,$$
$$S^{**} \xrightarrow{k_n'} \text{nonradiative decay},$$
$$S^{**} + S \xrightarrow{k_q'} \text{self-quenching},$$

where S^{**} denotes another electronic state. Again this mechanism does not contain electronic quenching processes of S^* and S^{**} to explain the leveling off of emission intensity at high pressures of M. This mechanism leads to the following equations 3 and 4.

$$I_0/I_f = 1 + [M]/(A+B[M]), \quad (3)$$

where

$$A = (k_r+k_q[S])/k_m \quad \text{and}$$
$$B = k_m'(k_r+k_q[S])/\{k_m(k_n'+k_q'[S])\},$$
$$1/I_f = \{k_q+(k_r+C[M])/[S]\}/(\alpha k_r), \quad (4)$$

where

$$C = k_m(k_n'+k_q'[S])/(k_n'+k_q'[S]+k_m'[M]).$$

Equation 4 can be approximated by Eq. 4', when

$$k_q'[S] \ll k_n' + k_m'[M], \quad (5)$$

$$1/I_f = [\{k_q+k_q'k_mk_m'[M]^2/(k_n'+k_m'[M])^2\} + \{k_r+k_mk_n'[M]/(k_n'+k_m'[M])\}/[S]]/(\alpha k_r). \quad (4)'$$

Equations 3 and 4' can explain the experimental results well. Fitting these equations to the experimental results, the quantities on the left-hand sides of the following equations can be experimentally determined.

$$k_m = (k_r+k_q[S])/A, \quad (6)$$

$$(k_n'+k_q'[S])/k_m' = A/B, \quad (7)$$

$$k_n'/k_m' = [M][k_m[M]/\{k_r(IR-1)\}-1]^{-1}, \quad (8)$$

$$k_q'/k_m' = k_mk_q[M]^2(SR-1)/\{k_m[M]-k_r(IR-1)\}^2, \quad (9)$$

where IR and SR are respectively the ratios of the intercept and the slope of the self-quenching in the presence of foreign gas of [M] to those in the absence of it. It should be noted that the quantity of $(k_n'+k_q'[S])/k_m'$ can be obtained by the two independent ways, one with Eq. 7 and the other with a combination of Eqs. 8 and 9. The results of application of these equations to the data of (110) band are compared for the three gases in Table 2. It can be seen that the condition (5) is met and that Eqs. 7—9 are self-consistent. The results of application of Eqs. 6 and 7 to other levels are summarized in Table 3. It seems that k_m is smaller than k_q by an order and is an increasing function of vibrational energy.

Finally, by adding vibrational relaxation to the above mechanism, we have a mechanism that can explain all the three features. In this case, the quantities k_m and $(k_n'+k_q'[S])/k_m'$ in Table 3 must be interpreted as some sort of weighted averages over several levels.

In quenching by N_2, additional weak electronic quenching of S* and/or S** must be operating because continuous decrease of I_f was observed above 200 Torr as seen in Fig. 6. The recovery of I_f at high pressures observed in quenching by He (Fig. 4) cannot be explained by the proposed mechanism. The comparison of the quenching rate constant by Ar reported by Okabe with the k_m value of the present work is meaningless because Okabe's value was calculated with I_0/I_f at 400 Torr of Ar assuming Stern-Volmer mechanism. However, I_0/I_f values themselves in the two works coincide with each other within an experimental error.

Since the quantum beat in the fluorescence decay of $\tilde{C}(^1B_2)$ state due to the weak vibronic coupling of the state to the ground electronic state $\tilde{X}(^1A_1)$ has been observed,[12] the nonemitting state S** invoked in the proposed mechanism might be the ground state. To identify S** state, kinetic studies of $SO_2(^1B_2)$ in the presence of foreign gas are needed.

Table 2. The results of application of the proposed mechanism to (110) band

Gas M	k_m	$(k_n'+k_q'[S])/k_m'$	k_n'/k_m'	$k_q'[S]/k_m'$
	10^{-10} cm^3 molecule^{-1} s^{-1}	10^{18} molecule cm^{-3}		
He	0.67	1.0	1.0	0.06
Ar	0.91	1.4	1.3	0.16
N_2	1.3	0.91	0.86	0.14

$k_r=3.1\times10^7$ s^{-1} from Ref. 11. $k_q=1.25\times10^{-9}$ cm^3 molecule^{-1} s^{-1} calcd from Q in Table 3.

The author wishes to thank Professors Shin Sato and Shigeru Tsunashima of Tokyo Institute of Technology and Dr. Shigeyoshi Arai of the Institute of Physical and Chemical Research for helpful discussions and encouragements.

References

1) Y. Hamada and A. J. Merer, *Can. J. Phys.*, **52**, 1443 (1974).
2) R. J. Shaw, J. E. Kent, and M. F. O'Dwyer, *J. Mol. Spectrosc.*, **82**, 1 (1980).
3) E. K. C. Lee, B. G. MacDonald, D. L. Holtermann, and R. Nanes, *J. Photochem.* **17**, 495 (1981).
4) H. Watanabe, Y. Hyodo, S. Tsuchiya, and S. Koda, *Chem. Phys. Lett.*, **81**, 439 (1981).
5) J. Duchesne and B. Rosen, *J. Chem. Phys.*, **15**, 631 (1947).
6) G. Herzberg, "Electronic Spectra of Polyatomic Molecules," Van Nostrand, Princeton (1966), p. 605.

Table 3. Self-quenching constants and the results of application of the proposed mechanism

Band	Self-quenching const Q[a]	k_m[b]			$(k_n'+k_q'[S])/k_m'$[c]		
		He	Ar	N_2	He	Ar	N_2
220.6 nm	—	—	—	—	1.1	1.4	—
222.3 nm	3.2	2.4	2.0	3.8	0.90	1.9	0.93
224.2 nm	2.3	1.5	2.7	2.7	1.1	1.5	0.85
(120)	1.5	0.88	1.3	1.9	1.5	1.6	0.91
(102)	1.9	—	—	—	—	—	—
(110)	1.3	0.67	0.91	1.3	1.0	1.4	0.91
(100)	1.1	0.53	0.77	1.2	0.86	1.1	0.62
(010)	1.1	—	—	—	0.90	1.8	—
(000)	1.0	—	—	—	0.60	0.90	—

a) Q/Torr$^{-1}=3.22\times10^{16}$ k_q/k_r. Error±10%. b) Calculated with Eq. 6. In 10^{-10} cm^3 molecule^{-1} s^{-1}. k_r's are taken from Ref. 11. c) Calculated with Eq. 7. In 10^{18} molecule cm^{-3}. [S]$\approx2.6\times10^{16}$ molecule cm^{-3}.

7) J. C. D. Brand, P. H. Chiu, and A. R. Hoy, *J. Mol. Spectrosc.*, **60**, 43 (1976).
8) J. C. D. Brand, D. R. Humphrey, A. E. Douglas, and I. Zanon, *Can. J. Phys.*, **51**, 530 (1973).
9) J. C. D. Brand and K. Srikameswaran, *Chem. Phys. Lett.*, **15**, 130 (1972).
10) H. Okabe, *J. Am. Chem. Soc.*, **93**, 7095 (1971).
11) Man-Him Hui and S. A. Rice, *Chem. Phys. Lett.*, **17**, 474 (1972).
12) W. Sharfin, M. Ivanco, and S. C. Wallace, *J. Chem. Phys.*, **76**, 2095 (1982).
13) H. Okabe, "Photochemistry of Small Molecules," Wiley-Interscience (1978).
14) H. Okabe, P. L. Splitstone, and J. J. Ball, *J. Air Pollution Control Assoc.*, **23**, 514 (1973).
15) The relative efficiencies (including the transmittance of the cell window) determined by compaison with thermopile data were 1:1:0.9:0.4 at 400, 350, 300, and 250 nm, respectively.
16) Weak bands buried were observed around 260 and 380 nm.
17) For the comparison, the quenching of $B(^1B_1)$ state excited at 285 nm measured for argon. The plot similar to Figs. 4—6 showed a straight line with argon pressure up to 80 Torr. The quenching rate constant obtained was 0.6×10^{-10} cm^3 molecule^{-1} s^{-1} which is compared to the value 0.5×10^{-10} reported by Mettee.[18]
18) H. D. Mettee, *J. Phys. Chem.*, **73**, 1071 (1969).